Engineering Computations

Numerical algorithm of reinforced concrete lining cracking process for pressure tunnels

Wei Zhang, Beibing Dai, Zhen Liu, Cuiying Zhou,

Article information:

To cite this document:
Wei Zhang, Beibing Dai, Zhen Liu, Cuiying Zhou, (2018) "Numerical algorithm of reinforced concrete lining cracking process for pressure tunnels", Engineering Computations, Vol. 35 Issue: 1, pp.91-107, https://doi.org/10.1108/EC-11-2016-0394
Permanent link to this document:
https://doi.org/10.1108/EC-11-2016-0394

Numerical algorithm of reinforced concrete lining cracking process for pressure tunnels

Wei Zhang
College of Water Conservancy and Civil Engineering, South China Agricultural University, Guangzhou, China and Research Center for Geotechnical Engineering and Information Technology, Sun Yat-sen University, Guangzhou, China, and

Beibing Dai, Zhen Liu and Cuiying Zhou
Research Center for Geotechnical Engineering and Information Technology, Sun Yat-sen University, Guangzhou, China

Received 20 November 2016
Revised 8 May 2017
Accepted 25 June 2017

Abstract

Purpose – The cracking of a reinforced concrete lining has a significant influence on the safety and leakage of pressure tunnels. This study aims to develop, validate and apply a numerical algorithm to simulate the lining cracking process during the water-filling period of pressure tunnels.

Design/methodology/approach – Cracks are preset in all lining elements, and the Mohr–Coulomb criterion with a tension cutoff is used in determining whether a preset crack becomes a real crack. The effects of several important factors such as the water pressure on crack surfaces (WPCS) and the heterogeneity of the lining tensile strength are also considered simultaneously.

Findings – The crack number and width increase gradually with the increase in internal water pressure. However, when the pressure reaches a threshold value, the increase in crack width becomes ambiguous. After the lining cracks, the lining displacement distribution is discontinuous and steel bar stress is not uniform. The measured stress of the steel bar is greatly determined by the position of the stress gauge. The WPCS has a significant influence on the lining cracking mechanism and should not be neglected.

Originality/value – A reliable algorithm for simulating the lining cracking process is presented by which the crack number and width can be determined directly. The numerical results provide an insight into the development law of lining cracks and show that the WPCS significantly affects the cracking mechanism.

Keywords Numerical simulation, Cracking, Lining, Pressure tunnel, Water pressure on crack surfaces

Paper type Research paper

1. Introduction

The pressure tunnel is an important underground structure in the hydropower station and generally lined by concrete. According to the present design principle, the cracks are allowed to occur in the concrete lining during the operation period. However, the crack width should be controlled to be an acceptable value (Hao *et al.*, 2004; Panthi, 2014). Cracks with large width may lead to unacceptable leakage in the pressure tunnel. Moreover, they may

The research is supported by the National Natural Science Foundationof China (NSFC) (Nos. 41530638, 41372302), High level talent project in Guangdong Province (No. 20143900042010003), and Technology Program Funding of Guangzhou (No. 201605030009).

Engineering Computations
Vol. 35 No. 1, 2018
pp. 91-107

0264-4401
DOI 10.1108/EC-11-2016-0394

also endanger the safety of pressure tunnel structure and the seepage stability of the surrounding rock. Therefore, the study of the lining cracking process in the pressure tunnel is of great significance.

Previous studies have shown that as the pressure tunnel is an underground structure, the mechanical properties and crack mechanism of the concrete lining of the pressure tunnel are quite different from the structures above the ground. Considering the action of the surrounding rock mass, several theoretical and analytical studies on the lining cracking problem have been carried out (Simanjuntak *et al.*, 2013; Amorim *et al.*, 2014; Fernandez, 1994; Seeber, 1985a, 1985b). Many scholars have developed different analytical formulas to describe the cracks in pressure tunnels (Darwin and Scanlon, 1986; Schleiss, 1997a, 1997b, 1998).

Compared with the analytical method, the numerical method reflects the various complicated factors in actual engineering practice (Mang *et al.*, 2015; Zhang and Bui, 2015). Thus, in recent years, researchers mostly use numerical methods to study the pressure tunnels (Lin *et al.*, 2007; Feist *et al.*, 2009; Olumide and Marence, 2012; Wang *et al.*, 2013). Because of the complexity of the engineering practice, the cracking behavior of the pressure tunnel lining has been simulated in only a few studies (Bian *et al.*, 2016). In these studies, the cracks were simulated implicitly by an equivalent model (Zhou *et al.*, 2015; Cividini *et al.*, 2012) or a damage model (Bian *et al.*, 2009). One of the disadvantages of these models is that the actual crack distribution cannot be described, and thus the crack number and the crack width cannot be determined directly. As mentioned above, the crack width is an important parameter in pressure tunnel design. Moreover, after the lining cracks, the internal water in the pressure tunnel will penetrate into the cracks and generate the water pressure on crack surfaces (WPCS). The WPCS may greatly influence the cracking mechanism of pressure tunnel concrete lining. The presence of the WPCS is an important property of the pressure tunnels, in contrast with the highway tunnels. Unfortunately, the WPCS has not yet been considered in these studies.

After the construction of a pressure tunnel is completed, the tunnel has to be filled with water before the operation of the hydropower station. During the water-filling period, the internal water pressure increases gradually and this loading process leads to development of cracks in the concrete linings. The safety and leakage of pressure tunnels are affected by the final lining crack state. To study the mechanism underlying the lining cracking of pressure tunnels, this paper focuses on the lining cracking process during the water-filling period. It is assumed that the rock mass and intact concrete are impermeable, and thus the water pressure can be treated as a surface force and the simulation of the hydro-mechanical behavior in rock mass is not required. A numerical algorithm is presented to simulate the lining cracking process, by which the lining crack number and width can be solved directly. In this algorithm, the discrete crack model is used to simulate the cracks in the concrete lining. Cracks are presented in all lining elements, and the Mohr–Coulomb criterion with a tension cutoff is used to determine whether a preset crack becomes a real crack. The heterogeneity of the concrete lining tensile strength was described by a statistical distribution function. To determine the cracking sequence of the lining elements, the concept of load ratio is introduced. The load incremental method is used for simulating the loading process during the tunnel water-filling period and the iteration method for solving the non-linear problem. The developed algorithm was validated by comparing the numerical results with the analytical solutions and laboratory test results. Finally, the developed algorithm was used in simulating the lining cracking process for an actual pressure tunnel and some substantial findings were obtained.

2. Numerical model of pressure tunnel lining cracking

The numerical model of pressure tunnel mainly involves the model of concrete lining cracking, the model of the heterogeneity of concrete lining and the model of steel bar and

surrounding rock. The overall numerical model is shown in Figure 1. A detailed description about this model has been provided in the further sections.

2.1 Model of concrete lining cracking

The discrete crack model is used in simulating the lining cracks. In this model, the cracks are simulated directly, and the influence of the lining cracks on the structure can be truly described. The practice of pressure tunnel shows that the lining cracks under the internal water pressure are generally in the longitudinal direction (Hao *et al.*, 2004; Bian *et al.*, 2016). Thus, the cracks can be considered to be in radial direction for the plane strain problem. Therefore, the zero-thickness crack elements are preset along the radial edges of all lining elements, and the Mohr–Coulomb criterion with a tension cutoff is used in determining whether a preset crack becomes a real crack. Thus, the progressive lining cracking can be simulated. No hypotheses about the crack number and crack width are introduced beforehand. Thus, the crack number and crack width can be solved directly using the present model.

The four-node isoparametric element and four-node zero-thickness interface element are used, respectively, to model the intact concrete and preset crack. The Mohr–Coulomb criterion with a tension cutoff is used as the concrete cracking criterion. The tensile criterion is used when tensile failure occurs, while the Mohr–Coulomb criterion is used when the shear failure occurs. The tensile criterion is given by:

$$\sigma = \sigma_t, \tag{1}$$

and the Mohr–Coulomb criterion is:

$$\tau = c + \sigma tan\phi, \tag{2}$$

where τ and σ are, respectively, the shear and normal stress of the interface element, σ_t is the tensile strength, and c and ϕ are, respectively, the cohesion force and frictional angle of

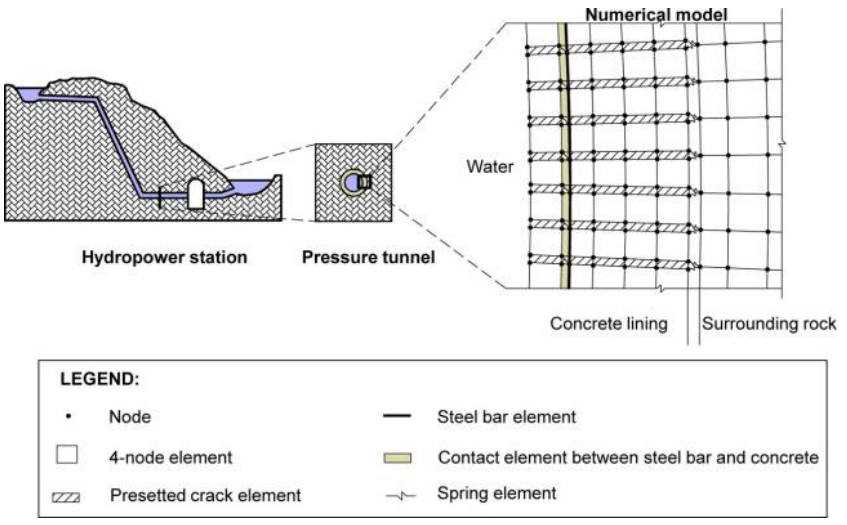

Figure 1.
Numerical model of pressure tunnel

the intact concrete. When $\sigma > \sigma_t$, tensile failure occurs. When $\tau > c + \sigma tan\phi$, shear failure occurs.

After the concrete lining cracks, internal water penetrates into the cracks and generates WPCS. A conventional model of pressure tunnel and a model with WPCS are compared in Figure 2.

The WPCS is directly applied on the crack, and thus, it significantly affects the lining cracking. The load of WPCS is given by:

$$\{f\} = \int_{\Gamma} \boldsymbol{N}^T p \boldsymbol{n}^T d\Gamma \tag{3}$$

where Γ denotes the edges of a crack element, $\boldsymbol{N}$ is the shape function of a crack element, p is the internal water pressure and $\boldsymbol{n}$ is the unit external normal vector. As the crack element is linear, one Gauss point is adopted for numerical integration. When the x-direction of the local coordinate system is along the length of the crack element, the load of WPCS can be derived as:

$$\{f\} = \frac{l}{2}[0 \quad -p \quad 0 \quad -p \quad 0 \quad p \quad 0 \quad p]^T \tag{4}$$

where l is the length of the crack element.

2.2 Model of the heterogeneity of concrete lining

Heterogeneity means spatial variation of mechanical parameters (such as elastic modulus, Poisson's ratio and strengths). In this paper, the heterogeneity of the concrete lining tensile strength was described by a statistical distribution function. In fact, the elastic modulus, cohesion strength, friction angle and other parameters of the concrete lining are all heterogeneous. However, in terms of the pressure tunnel, lining cracking is generally a kind of tensile failure, and the tensile strength of lining directly affects the lining cracking. Therefore, only the heterogeneity of the concrete lining tensile strength is considered.

There are many types of statistical distribution functions, such as exponential distribution, Gauss distribution and Weibull distribution. Among them, the Weibull distribution (Weibull, 1951) is based on the weakest link model and thus can better reflect the effect of material defects and stress concentration. Therefore, in this paper, the Weibull

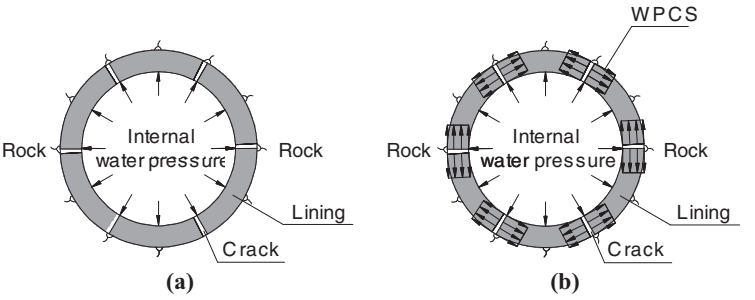

Figure 2.
Numerical model of pressure tunnel

Notes: (a) Traditional model; (b) model with WPCS

distribution is selected to describe the tensile strength heterogeneity of the concrete lining. The probability density function can be expressed as follows:

$$f(\sigma) = \frac{m}{\sigma_0}\left(\frac{\sigma}{\sigma_0}\right)^{m-1} exp\left(-\left(\frac{\sigma}{\sigma_0}\right)^{m}\right) \tag{5}$$

where σ is the probability variable value of the Weibull distribution, σ_0 the scale parameter and m the shape parameter. The parameter m defines the degree of material homogeneity and is also called the homogeneity index. The larger the parameter m is, the more homogeneous the material is. The parameter σ_0 is related to the average of the tensile strength and can be derived as:

$$\sigma_0 = \overline{\sigma_t}/\Gamma(1 + 1/m) \tag{6}$$

where $\overline{\sigma_t}$ is the average of the tensile strength and $\Gamma()$ the Γ function.

2.3 Model of steel Bar and surrounding rock

The bond slip model is adopted to model the steel reinforced concrete lining. A two-node bar element is used to model the steel bar and a 4-node contact element to model the bond slip between steel bar and concrete lining. This model is more consistent with the actual mechanical behavior of steel-reinforced concrete and can take into account the effect of the bond slip behavior after the lining cracks.

The stiffness matrix of the four-node contact element can be calculated as:

$$[K]^{e}_{cont} = \int_{l/2}^{l/2} [M]^{T}[\lambda][M]dx \tag{7}$$

where l is the length of the contact element, and $[M]$ and $[\lambda]$ are expressed as:

$$[M] = \frac{1}{2}\begin{bmatrix} -z_1 & 0 & -z_2 & 0 & z_2 & 0 & z_1 & 0 \\ 0 & -z_1 & 0 & -z_2 & 0 & z_2 & 0 & z_1 \end{bmatrix} \tag{8}$$

$$[\lambda] = \begin{bmatrix} \lambda_s & 0 \\ 0 & \lambda_n \end{bmatrix} \tag{9}$$

where λ_s and λ_n are, respectively, the shear and normal stiffness of the contact element, and z_1 and z_2 are given as:

$$z_1 = 1 - 2x/l \tag{10}$$

$$z_2 = 1 + 2x/l. \tag{11}$$

The stress of the contact element can be derived as:

$$\begin{Bmatrix} \tau \\ \sigma \end{Bmatrix} = [\lambda]\begin{Bmatrix} \Delta u \\ \Delta v \end{Bmatrix} \tag{12}$$

where τ and σ are, respectively, the shear and normal stress of the contact element, and Δu and Δv are, respectively, the shear and normal displacement difference.

For the bar element, the ideal elastic–plastic constitutive relation is used. When the steel bar stress $\sigma_b > [\sigma_b]$, the steel bar element yields. $[\sigma_b]$ is the steel bar yield stress. For the contact element, the elastic–brittle constitutive relation is used. When the shear stress of contact element $\tau > [\tau]$, the slip occurs. $[\tau]$ is the maximum bond stress obtained through laboratory testing.

The quadrilateral element is used to model the surrounding rock. As this study focuses on the lining cracking process, the elastic constitutive model is adopted for simplicity. Nevertheless, considering that the interaction force between lining and surrounding rock is generally in radial direction for circular tunnels, the normal rigid spring elements are used to model the interaction between the reinforced concrete lining and the surrounding rock.

3. Numerical implementation

The corresponding finite element mesh for the pressure tunnel is shown in Figure 1. This figure depicts the way in which all the aforementioned models can be combined. Note that all the preset crack elements, contact elements between the steel bar and the concrete lining and the spring elements between the surrounding rock and concrete in the mesh are zero-thickness/length elements. In other words, the corresponding nodes in the elements are coincident. To understand the association between the nodes, these elements are shown to possess a certain thickness/length in this figure.

To simulate the cracking process during the tunnel water-filling process, the load incremental method is applied. The internal water pressure is applied through several load steps. In each load step, the iteration method is used in solving the complicated non-linear problem, wherein concrete cracking, steel bar yielding and the bond slip between steel bar and concrete are considered. The detailed process is described below. The problem is firstly solved without considering the aforementioned non-linearity. Then, all types of elements are examined to see whether the failure occurs. If failure occurs, the element stiffness matrices are modified and the initial stress loading matrices of the failed elements are calculated. The initial stress loading matrices are then applied to calculate the structure response. The aforementioned procedure is repeated until no new failure element appears.

In terms of the contact element and the rigid spring, the stiffness factor values are considered to be high (e.g. 10^9 MPa/m) before failure. This is equivalent to the penalty method and ensures equal displacements of the related nodes. After failure, the stiffness factor values are considered to be low and positive (e.g. 10^{-5} MPa/m), to avoid numerical problem.

It should be mentioned that in each step, there may be more than one crack satisfying the cracking criteria. However, during the progressive loading process of the pressure tunnel, the stress re-distribution occurs immediately after one crack occurs. Therefore, to simulate the cracking process more concisely, we propose the rule that at the most a single crack occurs in each solving step. To consider the cracking subsequence of the elements, we define the load ratio to be the ratio between the calculated element stress and the allowable element stress according to the cracking criteria. According to the linear relationship between the element stress and the internal water pressure, the element with the minimum load ratio cracks first and is then taken to be the cracking element in the current solving step. The flow chart of the present algorithm is shown in Figure 3. On the basis of the algorithm, a corresponding calculation program has been developed.

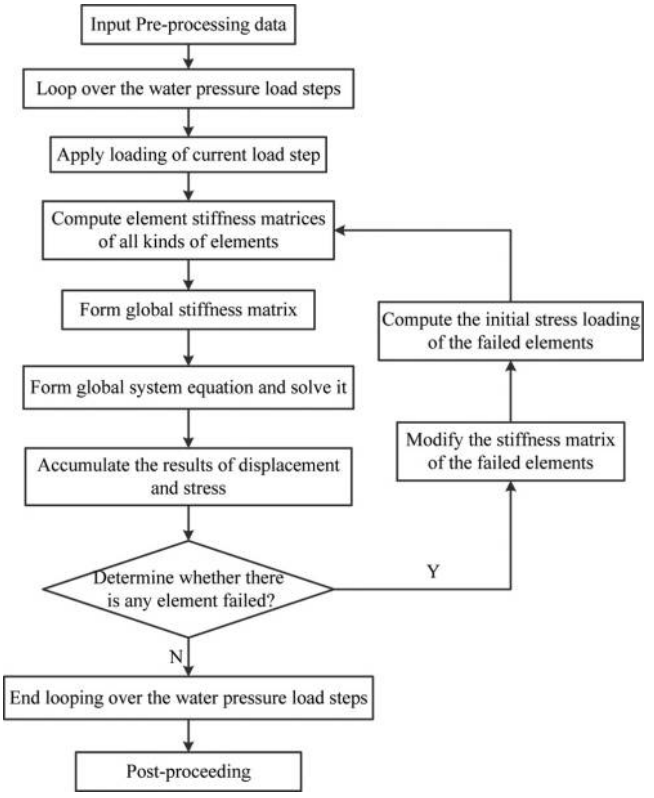

Figure 3.
Flow chart of the present algorithm

4. Verification examples

4.1 Pressure tunnel with intact lining

This example considers a circular pressure tunnel lined by a reinforced concrete. The internal diameter of the lining is 6.2 m, and the thickness 0.6 m. The diameter of the steel bar is 16 mm, and the spacing 200 mm. The elastic modulus of the concrete lining is E_c = 28 GPa and the Poisson's ratio μ_c = 0.167. The elastic modulus of the surrounding rock is E_r = 20 GPa and the Poisson's ratio μ_c = 0.25. The internal water pressure of the pressure tunnel is P = 1 MPa. Assuming that the lining is intact, this problem can be analytically solved according to elastic mechanics. The derivation procedure is as follows:

Under the internal and external pressure, the radial displacement at the external surface of the thick cylinder can be calculated as (Schleiss, 1986):

$$u_1 = \frac{r_2(1+\mu_c)}{E_c}\left[\frac{2(1-2\mu_c)}{t^2-1}P - \frac{1+(1-2\mu_c)t^2}{t^2-1}Q\right] \tag{13}$$

where P and Q are, respectively, the pressure applied on the internal and the external surfaces of the lining; $t = r_2/r_1$, where r_1 and r_2 are, respectively, the radii of the internal and external surfaces of the lining. The radial displacement of the infinite rock with the radial pressure Q can be calculated as:

$$u_2 = Qr_2 \frac{1+\mu_r}{E_r} \tag{14}$$

According to the displacement consistency at the interface between the concrete lining and the surrounding rock, $u_1 = u_2$; the pressure applied on the external surface of the lining can be calculated as:

$$Q = A/B \tag{15}$$

where:

$$A = \frac{2r_2(1+\mu_c)(1-2\mu_c)P}{Ec(t^2-1)} \tag{16}$$

$$B = r_2 \frac{1+\mu_r}{E_r} + \frac{r_2(1+\mu_c)(1+(1-2\mu_c)t^2}{Ec(t^2-1)} \tag{17}$$

Thus, the radial displacement at the lining internal surface is:

$$u_i = \frac{r_1(1+\mu_c)}{E_c}\left[\frac{(1-2\mu)+t^2}{t^2-1}P - \frac{2t^2(1-\mu)}{t^2-1}Q\right] \tag{18}$$

The circumferential stresses at the internal and external surfaces are, respectively, as follows:

$$\begin{aligned} \sigma_i &= \frac{r_1^2+r_2^2}{r_2^2-r_1^2}P - \frac{2r_2^2}{r_2^2-r_1^2}Q \\ \sigma_o &= \frac{2r_1^2}{r_2^2-r_1^2}P - \frac{r_1^2+r_2^2}{r_2^2-r_1^2}Q \end{aligned} \tag{19}$$

According to the displacement consistency conditions, the steel bar stress can be approximately calculated as:

$$\sigma_s = E_s u_i / r_1 \tag{20}$$

where E_s is the elastic modulus of the steel bar and considered to be 2.1×10^5 MPa in this study.

The present algorithm was used for analyzing this problem. For the computational mesh, the number of nodes is 5,605, the number of quadrilateral elements 3,905, the number of preset crack elements 1,920, the number of steel bar elements 160, the number of contact elements between the steel bar and the concrete is 160 and the number of spring elements between the concrete and the surrounding rock is 320.

Because all the preset crack elements did not meet the cracking criteria, no crack appeared in the lining, and the slip between steel bar and concrete did not appear either. The numerical results were compared with the analytical solutions, as shown in Table I. It can be observed that the displacement at the internal and external surfaces of the lining, the lining stresses and the steel bar stress are all in good agreement with the analytical solutions. Thus, the correctness of the present algorithm is verified preliminarily.

4.2 Laboratory test of pressure tunnel

In this example, a laboratory test of pressure tunnel was simulated by the present algorithm. Shen (2010) carried out a pressure tunnel laboratory test on a large scale with real internal water pressure, to study the mechanical properties of the pressure tunnel. The load of internal water pressure was simulated by the real water instead of a battery of hydraulic jacks; the test results have taken into account the effect of the WPCS.

In the laboratory test, the internal diameter of the tunnel was 0.8 m and the lining thickness 60 mm. The maximum water head in the test was 175 m. The tunnel lining was made of C20 concrete. The steel bar diameter was 8 mm, the spacing 100 mm and the thickness of the protective layer 7 mm. The grouted surrounding rock was simulated by a rectangular C10 concrete of dimensions 1.92 × 1.92 m. The class IV surrounding rock was simulated by a C10 concrete with air bubbles. The material parameters are shown in Table II.

For the computational mesh, the number of nodes is 4,949, the number of quadrilateral elements 2,891, the number of preset crack elements 1,440, the number of steel bar elements 160, the number of contact elements between the steel bar and the concrete 160 and the number of spring elements between the concrete and the surrounding rock 320. In the laboratory test, three cracks occurred in the 45°, 180° and 270° directions of the lining (0° for the top and positive for the clockwise direction). This suggests that the initial lining tensile strength at these positions was relatively low. This has been considered in the numerical simulation. To analyze the effect of the WPCS, numerical simulation without considering the WPCS was also carried out.

The displacement distribution of the concrete lining obtained by numerical simulation is shown in Figure 4. The maximum lining displacement is approximately 0.05 mm, and the displacement distribution is discontinuous along the cracks. The steel bar stress is shown in Figure 4(c). After the cracking of the lining, the stress of the steel bar near the crack increases significantly, and the maximum stress is about 78 MPa. Note that the stress distribution of the steel bar is not uniform, and the stress of the steel bar near the crack is much greater than that in the intact concrete. The concrete lining crack distribution is shown in Figure 4(d). Three cracks occurred successively

Item	Numerical result		Analytical result	Maximum error (%)
	Maximum	Minimum		
u_i (mm)	0.168	0.169	0.171	1.57
u_o (mm)	0.146	0.147	0.149	1.85
σ_i (MPa)	1.350	1.360	1.385	2.53
σ_o (MPa)	1.017	1.025	1.030	1.21
σ_s (MPa)	11.012	11.224	11.579	4.90

Table I. Comparison between the numerical and analytical results

Material	Elastic modulus (10^3 MPa)	Poisson's ratio
Lining	28	0.168
Steel bar	210	0.3
Grouted surrounding rock	20	0.168
Class IV surrounding rock	0.5	0.35

Table II. Material parameters of pressure tunnel laboratory test

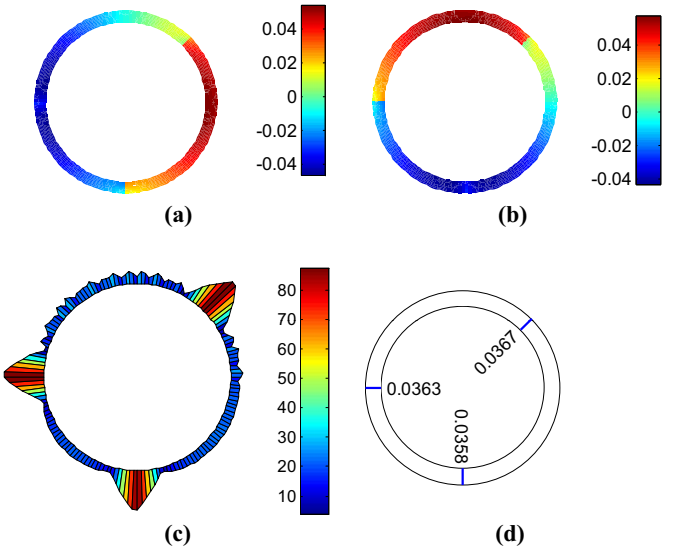

Figure 4.
Numerical results of the laboratory test

Notes: (a) x displacement distributions of concrete lining (unit: mm); (b) y displacement distributions of concrete lining (unit: mm); (c) stress of steel bar (unit: MPa); (d) crack distribution of concrete lining (unit: mm)

during the numerical computation. The maximum crack width is 0.0367 mm, and the average crack width 0.0363 mm.

The numerical results of the crack width and steel bar stress were compared with the laboratory results, as shown in Table III. In terms of the three cracks, the numerical results of the crack width and steel bar stress are similar, while the laboratory results obtained in the 180° direction are lower than those in other directions. The numerical results of the average crack width increase by 55 per cent when the WPCS is considered. It shows that the WPCS has a significant effect on the crack width and should not be neglected. Another evidence is that the numerical results with WPCS correspond well with the laboratory results, in comparison with the numerical results without WPCS. The numerical results show that the average steel bar stress increases by 12 per cent when WPCS is considered. The difference in steel bar stresses between

Table III.
Comparison of numerical results and laboratory results

	Laboratory result		Numerical result without WPCS		Numerical result with WPCS	
Position (°)	Crack width (mm)	Steel bar stress (MPa)	Crack width (mm)	Steel bar stress (MPa)	Crack width (mm)	Steel bar stress (MPa)
45	0.0357	41.66	0.0243	78.23	0.0367	87.66
180	0.0241	28.24	0.0228	75.70	0.0358	84.92
270	0.0332	99.59	0.0232	77.53	0.0363	86.83
Average	0.0310	56.50	0.0234	77.15	0.0363	86.47

the numerical and laboratory results is relatively large. The reason may be that the maximum steel bar stress is taken as the numerical result and the measured value in the laboratory test cannot be exactly the same as the maximum value. Because of the non-uniformity of the actual steel bar stress, the measured steel bar stress in the laboratory test is greatly influenced by the position of the stress gauge, and thus the measured values possess a certain randomness. It is impossible to install the stress gauge exactly at the crack beforehand because of the stochastic heterogeneity of lining. In general, the results of the numerical simulation agree with the laboratory results. The present algorithm is reliable to simulate the lining cracking process in the pressure tunnel. The WPCS has a significant effect on the cracking behavior and can be considered in the present algorithm.

5. Application to an actual pressure tunnel project

5.1 Project overview

The Huizhou pumped storage power station project is located near the Boluo county in the northeastern part of the Pearl River Delta, China. The total installed capacity is 2400 MW (8 × 300 MW), and the total cost is about US$ 1.2bn. The power station consists of two separate plants: Plant A and Plant B, with an installed capacity of 1200 MW (4 × 300 MW) for each plant. The layout of the tunnel and plant systems for each plant is similar, as shown in Figure 5. The reinforced concrete lining scheme is adopted for the high-pressure tunnel. The maximum static water head of the pressure tunnel is 627 m, one of the highest in the world. The pressure tunnel lining section is of annular shape. The internal diameter of the lining is 8.5 m and the thickness 0.6 m. The surrounding rock is slightly weathered or fresh granite, with a few small faults. Thus, the surrounding rock quality is generally good. Using the present algorithm, the pressure tunnel section with class III surrounding rock was analyzed, as shown in Figure 5. An image of the computation section is shown in Plate 1.

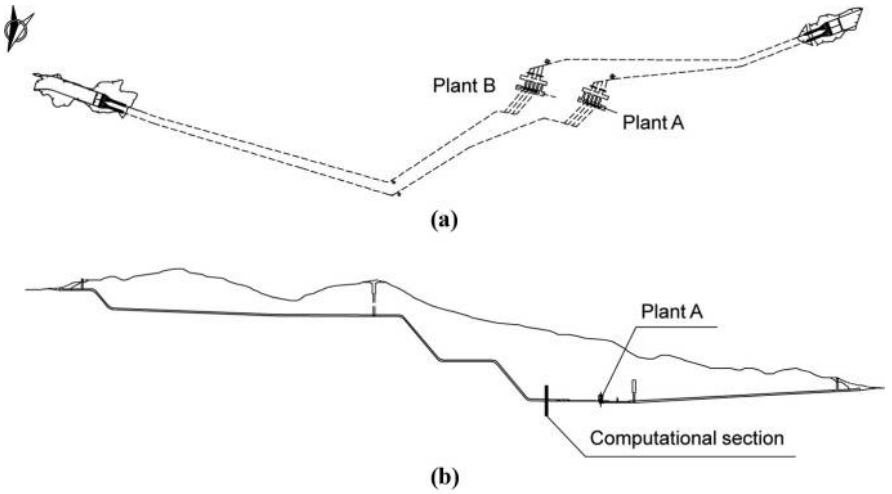

Figure 5.
Huizhou pumped storage power station project

Notes: (a) Plane layout; (b) longitudinal section layout

Plate 1.
Photo of pressure tunnel computational section

5.2 Numerical simulation and result analysis

For the computational mesh, the number of nodes is 10,309, the number of quadrilateral elements 5,634, the number of preset crack elements 3,840, the number of steel bar elements 320, the number of contact elements between the steel bar and concrete 320 and the number of spring elements between the concrete and the surrounding rock 640. The elastic modulus of the C25 lining is E_c = 28 GPa and the Poisson's ratio is μ_c = 0.167. The elastic modulus of the surrounding rock is E_r = 20 GPa and the Poisson's ratio μ_c = 0.25. The steel bar diameter is 25 mm, the spacing between the steel bars 125 mm and the thickness of the protective layer is 50 mm.

To consider the heterogeneity of the tensile strength of the concrete lining, the Monte Carlo method was used for creating random numbers. The Weibull distribution parameters were σ_t = 1.78 MPa and m = 3. The distribution of the tensile strength of the concrete lining is shown in Figure 8(a). The maximum internal water pressure and the WPCS were both 6.27 MPa. The total load was divided into eight equal parts and applied successively to simulate the pressure tunnel water-filling process.

The variation in the crack number and maximum crack width with the water head is shown in Figure 6. With the increasing water pressure, the crack number increases progressively, which indicates that the lining cracks appear successively. The maximum crack width also increases with the increasing water pressure. However, when the water head is greater than a certain value (about 200 m), the increase in the maximum crack width is not evident. It is because with the strength of the concrete lining being limited, when the water pressure reaches a certain value and further increases, new cracks appear progressively, which prevents further increase in the width of the existing cracks.

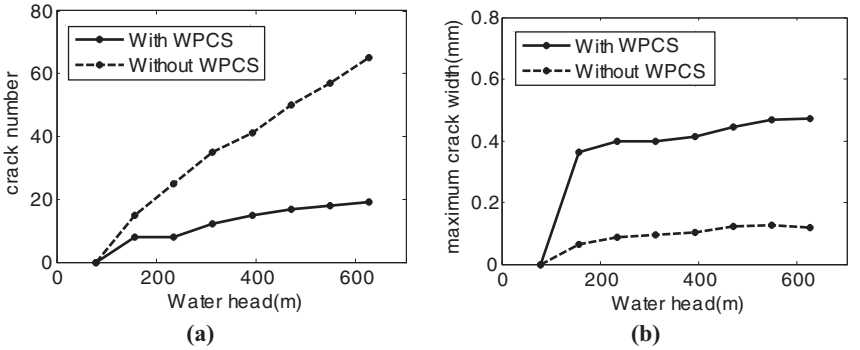

Figure 6. Variation of the crack number and average crack width with the water head

Notes: (a) Crack number; (b) average crack width

The radial displacement and crack distributions during the pressure tunnel water-filling process are shown in Figure 7. The variation process of the displacement and cracks can be observed clearly in this figure. It is found that the maximum displacement and crack number increase gradually with the increasing water pressure. Using the present algorithm, the lining cracking process with the increase in water pressure can be well simulated.

The final radial displacement distribution of concrete lining is shown in Figure 8(b). The maximum radial displacement is about 1.47 mm. The displacement distribution is discontinuous along the cracks as the lining cracks. The final stress of steel bar is shown in Figure 8(c). After the lining cracks, the stress of the steel bar near the crack increases significantly, and the maximum stress is about 190 MPa. Note that the steel bar stress distribution is not uniform, and the stress of the steel bar near the crack is much greater than that in the intact concrete. The actual measured steel bar stresses of this pressure tunnel also showed that the steel bar stress distribution was not uniform.

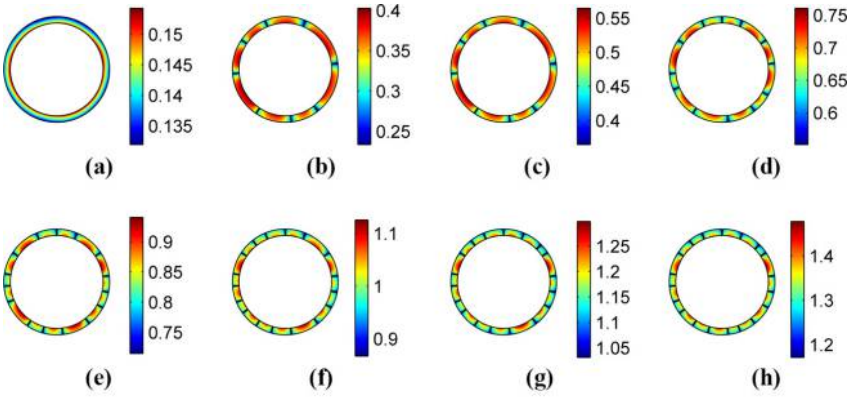

Figure 7. Radial displacement and crack distribution during the pressure tunnel water-filling process (unit: mm)

Notes: (a) $H = 78$ m; (b) $H = 157$ m; (c) $H = 235$ m; (d) $H = 314$ m; (e) $H = 392$ m; (f) $H = 470$ m; (g) $H = 549$ m; (h) $H = 627$ m

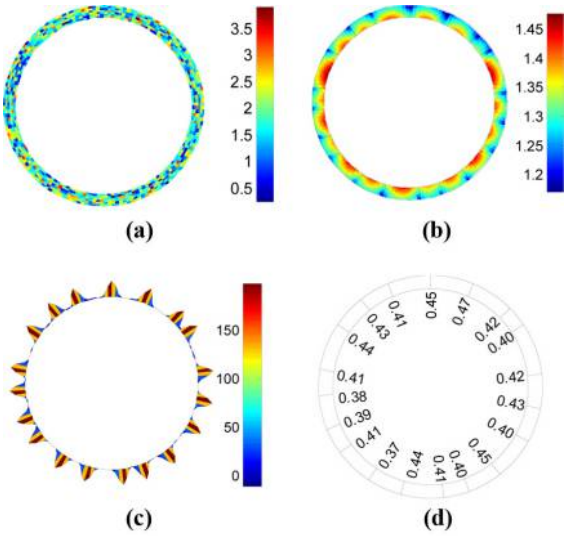

Notes: (a) Weibull distribution of lining tensor strength (unit: MPa); (b) radial displacement distributions of concrete lining (unit: mm); (c) stress of steel bar (unit: MPa); and (d) crack distribution of concrete lining (unit: mm)

Figure 8.
Final results of the computational section

The maximum steel bar stress was about 180 MPa, while the minimum value was negative, indicating compression stress. Thus, the steel bar stress is not uniform and the measured stress is greatly influenced by the position of the stress gauge. The measured value is large when the stress gauge is located near a crack, and it is small when the stress gauge is located near the middle of two nearby cracks. The final concrete lining crack distribution is shown in Figure 8(d). From this figure, we can observe that 19 cracks occurred successively during the water-filling process. The maximum crack width is 0.447 mm and the average crack width 0.406 mm. The spacing of cracks in a circumferential direction is roughly uniform.

5.3 Influence of the WPCS on the lining cracking process

To study the influence of the WPCS on the lining cracking process, numerical simulation was carried out without considering the WPCS. The other parameters are the same as those in Section 5.2. A comparison of the lining cracking process is made as shown in Figure 6. The final results of lining cracking are compared as shown in Table IV.

When considering the WPCS, the final crack number reduces from 65 to 19, and the crack width increases obviously. According to the inspection after the emptying of the pressure tunnel, the actual crack number in a cross section is generally not greater than 20. It can be deduced that it is more rational to consider the WPCS. The reason accounting for the less crack number is that after the lining cracks, the circumferential tensile stress of the lining reduces due to the presence of WPCS, and thus the concrete lining is not easy to crack. The reasons of greater crack width might be:

- the crack width is increased under the direct action of the WPCS; and
- under a constant total circumferential deformation, the crack width increases when the crack number reduces.

Therefore, it can be concluded that the WPCS has a significant influence on the lining cracking mechanism and should not be neglected.

It would be interesting to analyze the equivalent hydraulic conductivity of the lining after cracking, which has a significant influence on the leakage flow rate of pressure tunnels. The hydraulic conductivity along a crack can be calculated according to the cubic law (Witherspoon *et al.*, 1980; Zhang *et al.*, 2017a, 2017b):

$$k = \frac{\rho g e^2}{12\mu} \tag{21}$$

where ρ is the density of water, g the gravity acceleration, e the crack width and μ the dynamic viscosity of water. In this study, the density is $\rho = 10^3$ kg/m^3, the gravitational acceleration $g = 9.8$ m/s^2 and the viscosity $\mu = 10^{-3}$Pa · s. According to the number of cracks and assuming that the intact concrete is impermeable compared with the cracks, the equivalent hydraulic conductivity of the lining can then be obtained as follows:

$$\tilde{k} = \frac{n\rho g e^3}{12\mu\pi D} \tag{22}$$

where n is the number of cracks and D the lining diameter. According to equation (22), the equivalent hydraulic conductivity of the lining is 1.60×10^{-6} m/s when WPCS is neglected, while it is 4.21×10^{-5} m/s when WPCS is considered. It is clear that the equivalent hydraulic conductivity and the flow rate would be underestimated if the WPCS is neglected.

6. Conclusions

This study, while aiming to provide a direct solution of the number and width of the lining cracks, presents a numerical algorithm to simulate the cracking process of reinforced concrete lining for pressure tunnels. In contrast with the previous research, the discrete crack model is applied. The number and width of the lining cracks can be directly solved, by simultaneously considering the effect of several important factors, such as the WPCS and the heterogeneity of the lining tensile strength. The present algorithm can better capture the mechanical properties of the pressure tunnel and help provide a better insight into its working mechanism.

The numerical results show that with the increase in water pressure, the lining cracks appear progressively and the crack width gradually increases. However, when the water head reaches a certain value, the increase in crack width is not evident, while the crack

	Without WPCS	With WPCS
Maximum crack width (mm)	0.12	0.473
Average crack width (mm)	0.093	0.417
Crack number	65	19
Total width of cracks (mm)	6.405	7.92

Table IV. Comparison of the final results of lining cracking

number increases further. After the lining cracks, the lining displacement distribution is discontinuous and the steel bar stresses are not uniform. The steel bar stress near a crack is much greater than that in the intact concrete, due to which the steel bar stress is not uniform and the measured value is to a great extent determined by the position of the stress gauge. Moreover, the WPCS has a significant influence on the lining cracking mechanism and should not be neglected. When the WPCS is considered, the final crack number reduces considerably and the crack width evidently increases.

References

Amorim, D.L.N.D.F., Proenca, S.P.B. and Flrez, L.J. (2014), "Simplified modeling of cracking in concrete: application in tunnel linings", *Engineering Structures*, Vol. 70, pp. 23-35.

Bian, K., Xiao, M. and Chen, J. (2009), "Study on coupled seepage and stress fields in the concrete lining of the underground pipe with high water pressure", *Tunnelling & Underground Space Technology*, Vol. 24, pp. 287-295.

Bian, K., Liu, J., Xiao, M. and Liu, Z. (2016), "Cause investigation and verification of lining cracking of bifurcation tunnel at Huizhou pumped storage power station", *Tunnelling & Underground Space Technology*, Vol. 54, pp. 123-134.

Cividini, A., Contini, A., Locatelli, L. and Gioda, G. (2012), "Investigation on the cause of damages of a deep tunnel", *International Journal of Geomechanics*, Vol. 12 No. 6, pp. 722-731.

Darwin, D. and Scanlon, A. (1986), "Cracking of members in direct tension", *ACI Journal*, Vol. 83, pp. 3-12.

Feist, C., Aschaber, M. and Hofstetter, G. (2009), "Numerical simulation of the load–carrying behavior of RC tunnel structures exposed to fire", *Finite Elements in Analysis & Design*, Vol. 45 No. 12, pp. 958-965.

Fernandez, G. (1994), "Behavior of pressure tunnels and guidelines for liner design", *Journal of Geotechnical Engineering*, Vol. 120 No. 10, pp. 1768-1791.

Hao, Y., Duan, L., Hao, Z., *et al.* (2004), *Specification for Design of Hydraulic Tunnel*, Beijing.

Lin, M.L., Chung, C.F., Jeng, F.S. and Yao, T.C. (2007), "The deformation of overburden soil induced by thrust faulting and its impact on underground tunnels", *Engineering Geology*, Vol. 92 Nos 3/4, pp. 110-132.

Mang, C., Jason, L. and Davenne, L. (2015), "A new bond slip model for reinforced concrete structures: validation by modelling a reinforced concrete tie", *Engineering Computations*, Vol. 32 No. 7, pp. 1934-1958.

Olumide, B.A. and Marence, M. (2012), "A finite element model for optimum design of plain concrete pressure tunnels under high internal pressure", *International Journal of Engineering and Technology*, Vol. 2, pp. 676-683.

Panthi, K.K. (2014), "Norwegian design principle for high pressure tunnels and shafts: its applicability in the Himalaya", *Hydro Nepal: Journal of Water, Energy and Environment*, Vol. 14, pp. 36-40.

Schleiss, A.J. (1986), "Design of previous pressure tunnels", *International Water Power and Dam Construction*, Vol. 38 No. 5.

Schleiss, A.J. (1997a), *Design of Concrete Linings of Pressure Tunnels and Shafts for External Water Pressure*, Tunnelling ASIA, New Delhi, pp. 291-300.

Schleiss, A.J. (1997b), "Design of reinforced concrete linings of pressure tunnels and shafts", *Hydropower Dams*, Vol. 4, pp. 88-94.

Schleiss, A.J. (1998), "Design criteria applied for the lower pressure tunnel of the North Fork Stanislaus river hydroelectric project in California", *Rock Mechanics and Rock Engineering*, Vol. 21, pp. 161-181.

Seeber, G. (1985a), "Power conduits for high–head plants: part one", *International Water Power & Dam Construction*, Vol. 37, pp. 50-54.

Seeber, G. (1985b), "Power conduits for high–head plants: part one", *International Water Power & Dam Construction*, Vol. 37, pp. 95-98.

Shen, W. (2010), "Test research on the limiting crack design of hydraulic reinforced concrete tunnel lining", *Water Resources and Power*, Vol. 28, pp. 78-81.

Simanjuntak, T.D.Y.F., Marence, M., Mynett, A.E. and Schleiss, A. (2013), "Mechanical–hydraulic interaction in the cracking process of pressure tunnel linings", *International Journal on Hydropower and Dams*, Vol. 20 No. 5, pp. 112-119.

Wang, T., Wu, H., Li, Y., Gui, H., Zhou, Y., Chen, M., Xiao, X., Zhou, W. and Zhao, X. (2013), "Stability analysis of the slope around flood discharge tunnel under inner water exosmosis at Yangqu hydropower station", *Computers & Geotechnics*, Vol. 51, pp. 1-11.

Weibull, W. (1951), "A statistical distribution function of wide applicability", *Journal of Applied Mechanics ASME*, Vol. 18, pp. 293-297.

Witherspoon, P.A., Wang, J.S.Y., Iwai, K. and Gale, J.E. (1980), "Validity of cubic law for fluid flow in a deformable rock fracture", *Water Resources Research*, Vol. 16 No. 6, pp. 1016-1024.

Zhang, W., Dai, B., Liu, Z. and Zhou, C. (2017a), "Modeling free-surface seepage flow in complicated fractured rock mass using a coupled RPIM-FEM method", *Transport in Porous Media*, Vol. 117 No. 3, pp. 443-463.

Zhang, W., Dai, B., Liu, Z. and Zhou, C. (2017b), "A pore-scale numerical model for non-Darcy fluid flow through rough-walled fractures", *Computers and Geotechnics*, Vol. 87, pp. 139-148.

Zhang, X. and Bui, T.Q. (2015), "A fictitious crack XFEM with two new solution algorithms for cohesive crack growth modeling in concrete structures", *Engineering Computations*, Vol. 32 No. 2, pp. 473-497.

Zhou, Y., Su, K. and Wu, H. (2015), "Hydro-mechanical interaction analysis of high pressure hydraulic tunnel", *Tunnelling & Underground Space Technology*, Vol. 47, pp. 28-34.

Corresponding author
Cuiying Zhou can be contacted at: ueit@mail.sysu.edu.cn